Tidal and subtidal fluctuations in temperature, salinity and pressure for the winter 1996 larval ingress experiment—Beaufort Inlet, NC

JACKSON O. BLANTON,[1] JULIE AMFT,[1] RICHARD A. LUETTICH JR,[2] JAMES L. HENCH[2] AND JAMES H. CHURCHILL[3]

[1]*Skidaway Institute of Oceanography, 10 Ocean Science Circle, Savannah, GA 31411, USA*
[2]*Institute of Marine Sciences, The University of North Carolina at Chapel Hill, 3431 Arendell Street, Morehead City, NC 28557, USA*
[3]*Woods Hole Oceanographic Institution, Clark Laboratory, Woods Hole, MA 02543, USA*

ABSTRACT

A multidisciplinary field experiment was conducted to compare water properties, larval abundances, and transport and retention processes at Beaufort Inlet and two channels leading to the estuarine nursery grounds. Temperature, salinity and subsurface pressure were monitored *in situ* for a six-week period during March and April 1996 in each channel. Intensive sampling was performed during two neap-tide periods when water mass conditions in the estuary were significantly different. Currents were stronger in the eastern channel during both experiments. Ebb currents were stronger than flood in both channels. Decreasing subtidal sea level appeared to account for the stronger ebb currents. Subtidal sea level in the inlet responded optimally to north–south (along the inlet axis) wind stress and along a line 15° clockwise of north–south. This direction closely parallels the channel axis of Core Sound and may provide an efficient conduit to carry large volumes of low-salinity Pamlico Sound water into the estuarine complex when winds blow south in this sector. The tidal stream in Beaufort Inlet sets up strong cross-inlet gradients by the advection on the east side of higher salinity shelf water and advection on the west side of Beaufort Inlet plume water. The axial fronts produced by differential advection of these two water masses might play some role in redistributing larvae present in one tidal stream to another.

Key words: estuaries, inlets, tidal transport, wind transport, larval transport

INTRODUCTION

Beaufort Inlet (Fig. 1) connects a complex of sounds and estuaries to the Atlantic Ocean. Two main channels distribute ocean waters into this complex: a western channel, which goes into the Port of Morehead City and Bogue Sound, and an eastern channel, which extends behind Shackleford Banks. A smaller channel extends off the western channel by Radio Island and into the town of Beaufort. Depths are generally less than 2 m, except in the main channels where depths can be as great as 8 m (Klavans, 1983). The main channel into the Port of Morehead City is dredged to a depth of between 12 m and 15 m.

The largest source of fresh water directly discharged into the system is the Newport River running into the western channel (Kirby-Smith and Costlow, 1989). This small river has monthly mean discharges which vary between 0.4 $m^3\ s^{-1}$ in August to 11.2 $m^3\ s^{-1}$ in January. One must recognize the significantly larger Neuse River as a potentially important source which can discharge fresh-water volumes an order of magnitude larger into Core Sound (Jennings *et al.*, 1970). In addition, the Neuse River can affect salinities in Core Creek, which can also discharge small volumes into the Newport River estuary (Logan, 1995).

Maximum tidal current speeds of about 1 m s^{-1} occur in the inlet pass between Bogue and Shackleford Banks, and generally decrease inland (Klavans, 1983). The tide enters the estuarine complex through Beaufort Inlet as a damped progressive wave the amplitude of which decreases along the western and eastern channels. There is a lag of about 1.7 h between high water and slack water in Beaufort Inlet. This compares with a 1.5-h lag calculated by a hydrodynamic model (Luettich *et al.*, 1999).

Wind stress can transport water into the complex not only through Beaufort Inlet but also through Core Sound at the south-western tip of Pamlico Sound (Pietrafesa and Janowitz, 1988). This fact complicates the response of sea level in the Beaufort Inlet vicinity,

Correspondence: Dr J. O. Blanton, Skidaway Institute of Oceanography, 10 Ocean Science Circle, Savannah, GA 31411, USA. E-mail: jack@skio.peachnet.edu
Received for publication 1 June 1998
Accepted for publication 4 January 1999

© 1999 Blackwell Science Ltd.

Figure 1. Location maps with geographical names and locations of instruments and ships. Dots in the right-hand panel denote the positions of anchored ships and the two moored instruments.

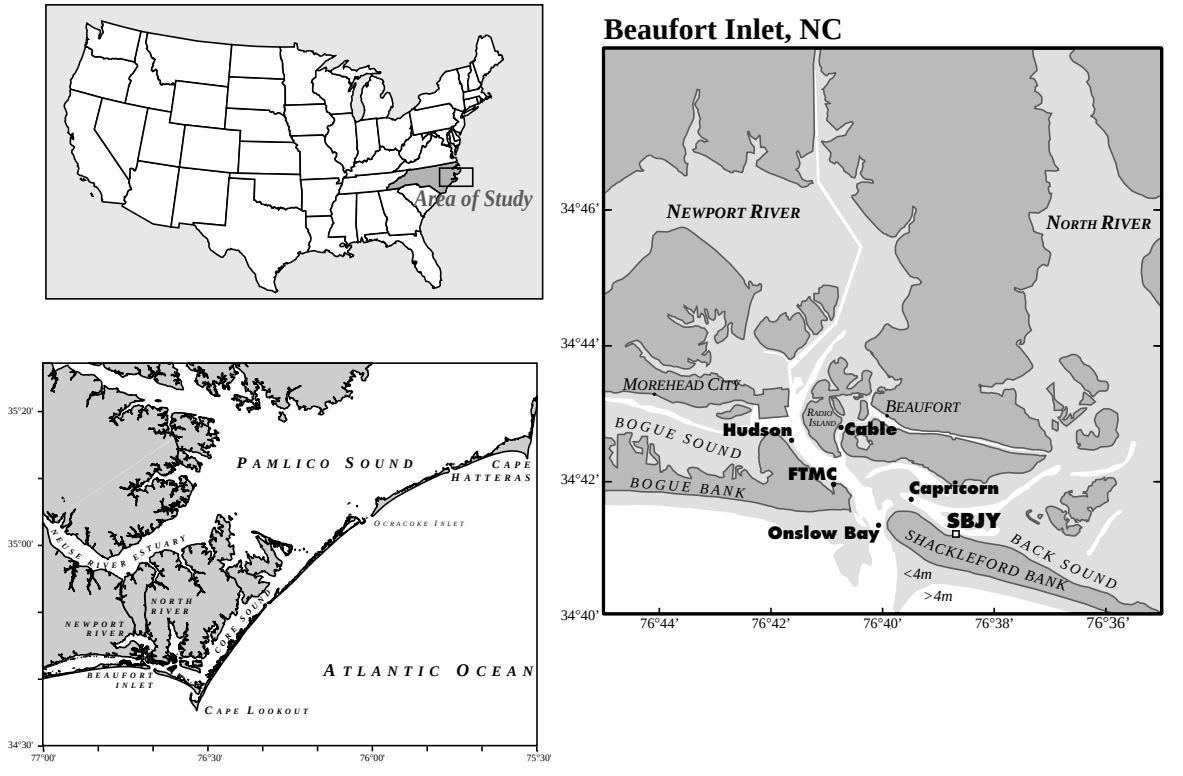

since wind stress from a variety of directions can increase or decrease the water level there (Janowitz and Pietrafesa, 1980; Hofmann *et al.*, 1981; Logan, 1995). This paper will show that oceanic water masses changed at the mouth of Beaufort Inlet in response to changes in wind stress direction.

A multidisciplinary field experiment was conducted during March 1996 to compare water properties, larval abundances, and transport and retention processes at Beaufort Inlet and in the main channels leading to the estuarine nursery grounds. Data were collected during two sampling periods of 25 h, by a fleet of two anchored and three mobile vessels. In addition, *in situ* instruments monitored temperature, salinity and subsurface pressure (SSP) for a period of six weeks.

This paper focuses on a description of the six-week time series and how the conditions that were encountered during the two intensive sampling periods fit into the longer-term framework. Reported separately are the results from a hydrodynamic and particle-tracking model (Luettich *et al.*, 1999), the volume flux studies using the acoustic Doppler current profiler (ACDP) data (Churchill *et al.*, 1999), and the larval abundance findings (Forward *et al.*, 1999).

FIELD SAMPLING PROGRAMME

Long time series

Instruments were placed on opposite sides of Beaufort Inlet on fixed platforms at Fort Macon (FTMC) and the north side of Shackleford Bank (SBJY) (Fig. 1). These instruments (Table 1) recorded *in situ* temperature, conductivity, SSP and uncalibrated optical backscatterance for the period 4 March–18 April 1996 at a 6-min sample rate. These data were complemented by hourly wind and other meteorological measurements at Cape Lookout (CLKN7), which is a Coastal-Marine Automated Network Station (C-MAN) operated by the National Oceanographic and Atmospheric Administration (NOAA).

Ships

Six sites were occupied for intensive measurements of physical oceanographic parameters and larval abundances (Table 1). Two ships (R/V Susan Hudson and R/V Capricorn) were moored for two consecutive tidal cycles under two neap-tide conditions: NEAP 1 on 13–14 March and NEAP 2 on 25–26 March. The

Table 1. SABRE winter 1996—instrument documentation and locations.

Station	Instrument depth (mab)	Water depth (m)	Instrument	Parameters	Period	Latitude (N) degree	Latitude (N) min	Longitude (W) degree	Longitude (W) min
R/V Susan Hudson (Duke University Marine Laboratory)									
HUDA	Profile	7.0	SBE	C,D,F1,Ob,T	1,2	34	42.18	76	41.16
HUDA	Profile	7.0	S4	D,V	1,2	34	42.18	76	41.16
HUDA	6.5	7.0	SC	C,T	1,2	34	42.18	76	41.16
HUDM	0.1	8.0	SC	C,Ob,P,T	1,2	34	42.21	76	41.22
HUDM	0.5	8.8	S4	V	2	34	42.21	76	41.22
R/V Capricorn (University of North Carolina)									
CAPA	Profile	5.9	S4	C,D,T,V	1,2	34	41.72	76	39.45
CAPM	0.1	6.6	SC	C,Ob,P,T	1,2	34	41.78	76	39.58
CAPM	0.5	6.6	S4	V	1,2	34	41.78	76	39.58
R/V Onslow Bay (National Oceanographic and Atmospheric Administration)									
ONSE	Profile	7.6	SBE	C,D,T	1,2	34	41.32	76	39.98
ONSC	Profile	17.6	SBE	C,D,T	1,2	34	41.34	76	40.05
ONSW	Profile	11.0	SBE	C,D,T	1,2	34	41.38	76	40.22
R/V Cable (National Oceanographic Atmospheric Administration)									
RADE	Profile	4.9	SBE	C,D,T	1,2	34	42.77	76	40.76
R/V Mytlus (Woods Hole Oceanographic Institution)									
SH	Profile	6.9	SBE	C,D,T	1,2	34	41.55	76	39.37
MHN	Profile	6.7	SBE	C,D,T	1	34	42.10	76	40.50
MHS	Profile	15.3	SBE	C,D,T	1	34	42.02	76	40.60
MHE	Profile	15.4	SBE	C,D,T	2	34	42.03	76	40.58
BC1	Profile	6.7	SBE	C,D,T	1	34	42.38	76	40.71
BC2	Profile	8.4	SBE	C,D,T	2	34	42.55	76	40.77
Moorings (Skidaway Institute of Oceanography)									
FTMC	2.7	5.5	SC	C,Ob,P,T	3	34	41.95	76	40.90
SBJY	1.2	2.5	SC	C,Ob,P,T	3	34	41.23	76	38.60
Weather Station (C-MAN) (National Oceanographic & Atmospheric Administration)									
CLKN7	Weather		C-MAN	A,B,W	3	34	37.30	76	31.50

Instrument depths are given as metres above bottom (mab). Codes used in the table are: Instrument: SBE = Sea-Bird Electronics CTD; SC = Sea-Bird Electronics SEACAT data logger; S4 = InterOcean Systems S4 current meter. Parameter codes: A = air temperature; B = barometric pressure; C = conductivity; D = depth; Fl = chlorophyll a fluorescence; Ob = optical back-scatterance; P = SSP; T = water temperature; V = current velocity; W = wind velocity. Time periods in EST are as follows: 1 = NEAP 1 anchor station: begins 03/13/96 at about 09:00 and ends 03/14/96 at about 12:00; 2 = NEAP 2 anchor station: begins 03/25/96 at about 11:00; ends 03/26/96 at about 15:00; 3 = long-term moorings: begins 03/04/96 at 15:00; ends 04/18/96 at 12:30.

R/V Susan Hudson monitored conditions in the western channel (between Beaufort Inlet and Morehead City); the R/V Capricorn similarly monitored in the eastern channel extending behind Shackleford Bank (Fig. 1). Half-hourly or hourly vertical profiles of current velocity, temperature and salinity were measured at each of the two sites (Table 1). Current profiles obtained with the InterOcean Systems S4 current meters (a sampling rate of 2 Hz averaged for 1 min at each level) were taken with vertical resolutions of 2 m in the west channel and 1 m in the east channel. Temperature and salinity were recorded independently with a SeaBird Electronics CTD on the R/V Hudson, but as part of the S4 data stream on the R/V Capricorn.

The vertical profile data were supplemented by a Sea-Bird Electronics SEACAT logger and an S4 current meter (Table 1) placed on the bottom near the two ships, which measured currents, temperature and salinity. The sampling rates for the SEACATS and S4s were 3 min and 30 s respectively.

Two other ships (R/V Onslow Bay and R/V Cable) measured vertical profiles of temperature and salinity and larval abundances during the two neap-tide periods (Table 1). The R/V Onslow Bay sampled at east, middle and west positions in the inlet throat. The R/V Cable sampled in the channel just east of Radio Island. In addition, the R/V Mytlus took CTD profiles at 3–4 fixed stations (Table 1) on a cruise track along which an ADCP obtained continuous current profiles (Churchill *et al.*, 1999).

EXTERNAL FORCING

Fresh-water discharge history

Discharge data from the Neuse River was used as an index of fresh-water discharge into the Beaufort Inlet estuarine system. Historical data (US Geological Survey 1996) (1983–96) indicate that the Neuse discharge has varied from a low of 10 $m^3\ s^{-1}$ in August 1983, to a maximum of 370 $m^3\ s^{-1}$ in September 1996. The February and March historical means are 120 $m^3\ s^{-1}$ and 170 $m^3\ s^{-1}$ respectively.

Daily discharges from January through March 1996 (Fig. 2(a)) varied from a low of about 50 $m^3\ s^{-1}$ (day 1) to a large discharge pulse of 250 $m^3\ s^{-1}$ in early February (day 37). This event followed a rainstorm on 27 January (Fig. 2(c)). Discharge slowly decreased afterwards to values of about 100 $m^3\ s^{-1}$. The accumulative effect of a month of higher-than-normal discharge would be to lower the salinity of this complex estuarine system. An abrupt salinity decrease was observed one month after the peak discharge in Morehead and Shackleford Channels on day 72 (12 March) (Fig. 2(b)). Although we suspect a cause-and-effect link between high discharge and the abrupt lowering of salinity in the channels, the mechanism that explains the abruptness of the decrease is obscure.

Wind stress at Cape Lookout

Throughout this paper, we specify wind direction as being that *from* which the wind is blowing. The field experiment was carried out at a time when the wind stress regime typically changed from one punctuated by north-easters (south-west stress) to one during which south-westerly winds (north-eastward stress) prevailed (Weber and Blanton, 1980). Wind velocity at Cape Lookout was resolved into east (x) and north (y) components and wind stress was calculated along these axes. An iterative method (Blanton *et al.*, 1989) was used to estimate wind velocity at a common level of 10 m before stress was calculated.

The wind stress data extended from 5 March to 18 April 1996 (Figs 3(a) and 3(b)). The principal axis was 57° (rotated counterclockwise from east). This places the component of maximum variance along a line running approximately from north-east to south-west. There were three occurrences during which wind stress exceeded 0.3 Pa. The first occurred from 8 to 13 March, during which a cold northerly wind exerted offshore stress.

The first neap-tide field experiment (13–14 March) was conducted immediately after this storm. The second high-stress period occurred between 19 and 22 March, when strong warmer winds blew out of the south-west. These winds exerted an upwelling-favour-

Figure 2. River discharge data, inlet salinity and rainfall comparisons for the period 1 January to 19 April 1996: (a) Neuse River discharge at Kinston, NC; (b) low-frequency variations in salinity in the east and west channels; (c) rainfall at Morehead City, NC.

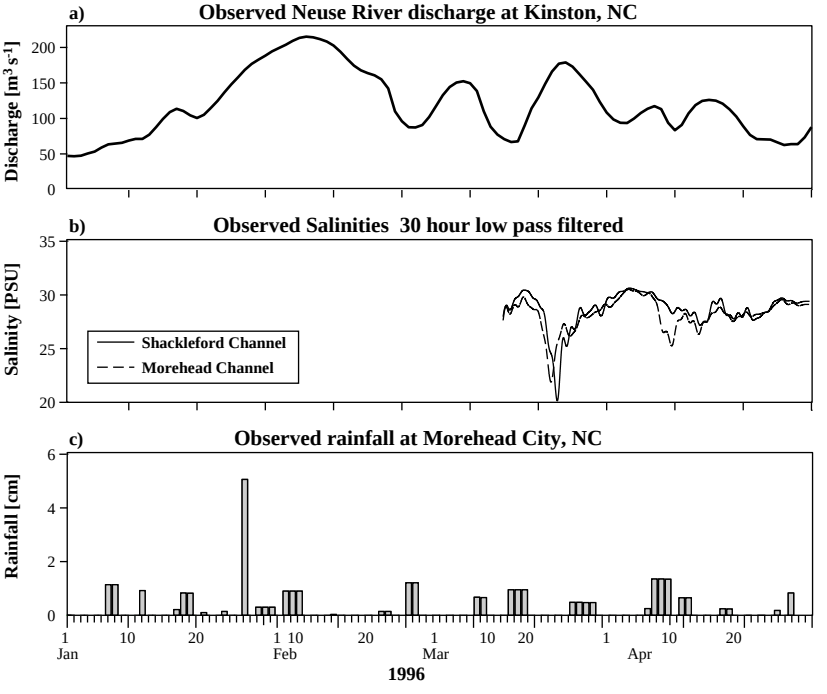

Figure 3. Hourly wind stress and subtidal frequency water level fluctuations in the east and west channels: (a) east, north stress component; (b) wind stress vectors; (c) SSP (as water level); (d) SSP difference between east and west channels. SSP data have been smoothed with a 30-h low pass filter. Numbered shaded areas denote regimes discussed in the text. The *y*-axis is aligned in a northerly direction for this and all subsequent vector plots.

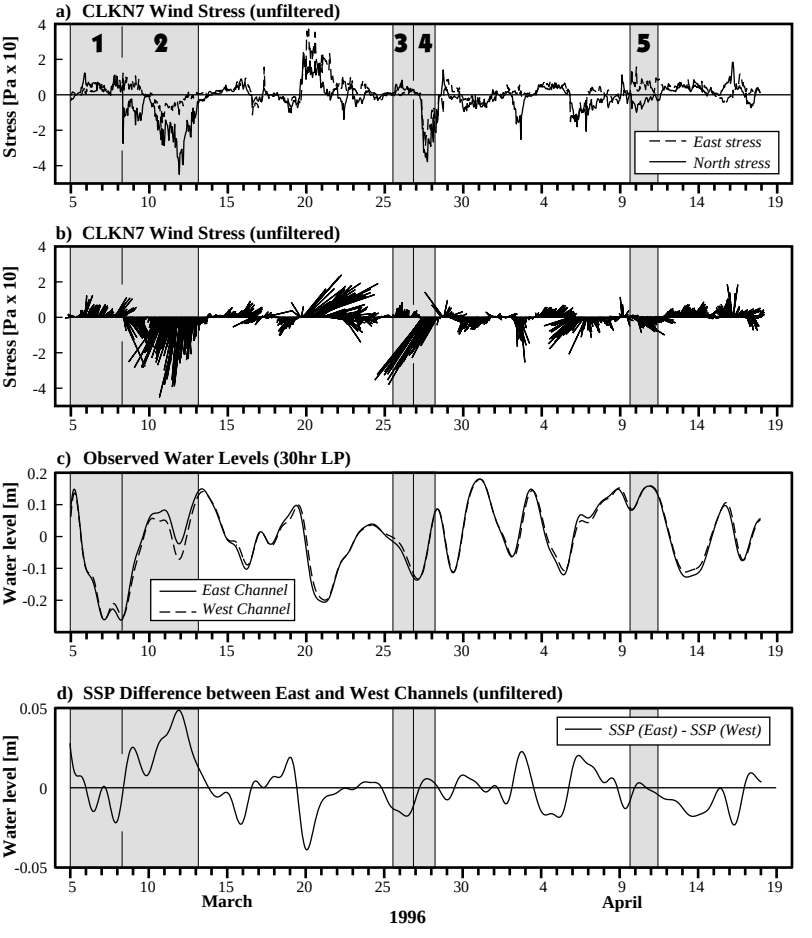

able stress in Onslow Bay. The second neap-tide field experiment (25–26 March) was conducted just after this event. Another strong north-easter occurred just after the second neap tide experiment on 27–28 March. Thus, the two neap-tide field experiments were conducted within about a day after two strong wind stress periods. The first followed a strong north-easter, while the second followed strong upwelling in Onslow Bay.

TEMPERATURE, SALINITY AND SSP CHANGES IN THE EAST AND WEST CHANNELS

Time series of temperature, salinity and SSP from the moored instruments were examined in the east and west channels in order to define the conditions that led into the times of the intensive sampling periods. Examination of this data set includes study of the response of sea level to wind stress and the corresponding tidal and subtidal fluctuations in temperature and salinity.

Sea-level response

Spectra of wind and sea level

The power spectral density of Cape Lookout wind stress and SSP are compared at several scales (Fig. 4). The wind stress and SSP reveal common energy peaks in the subtidal frequency band from 0.1 to 0.4 cycles per day (periods of 3–10 days). A secondary peak at slightly less than one cycle per day (about 25 h) occurs in the SSP, coinciding with diurnal tidal frequencies. The subtidal SSP fluctuations are overshadowed by more than an order of magnitude by the variance of the semidiurnal tide.

Tidal amplitude at semidiurnal and diurnal frequencies are slightly greater in the West (Morehead) Channel

Figure 4. Power spectra density: (a) wind stress at Cape Lookout; (b) SSP in the east and west channels; (c) same as (b) rescaled.

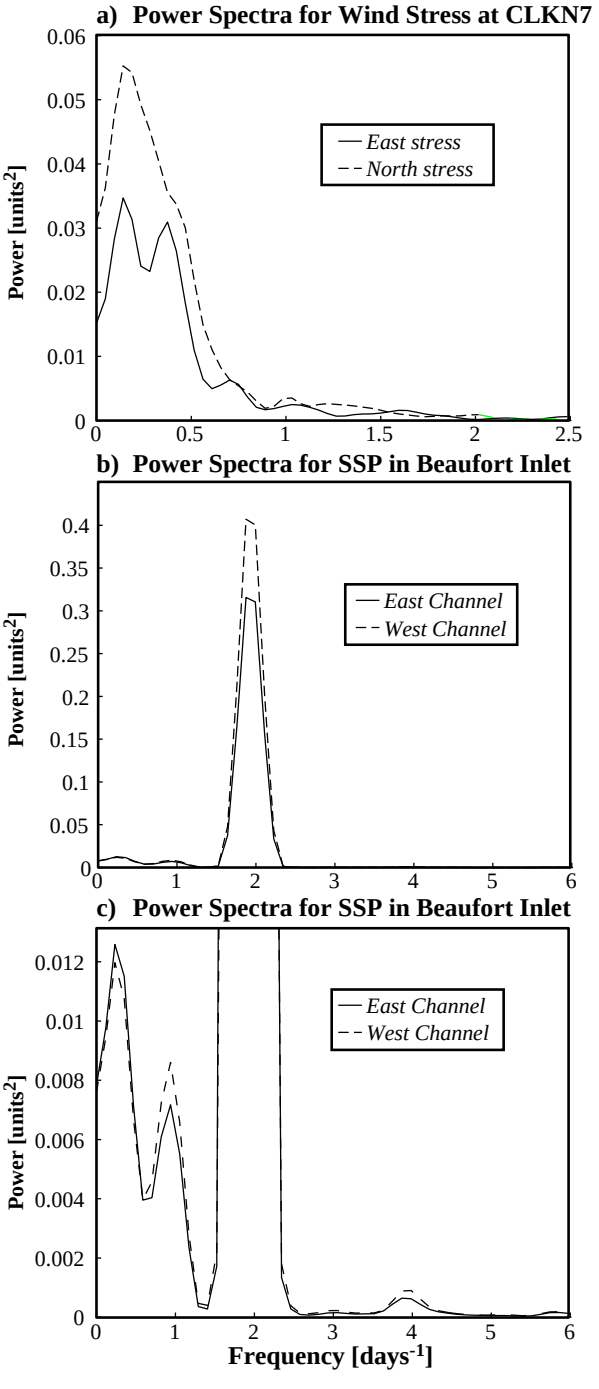

(Figs 4(b) and (c)), in agreement with the harmonic analyses discussed in the following section. However, the subtidal amplitudes (less than one cycle per day) are slightly greater in the east (Shackleford Channel).

Fort Macon and Shackleford tidal harmonics

Tidal currents provide most of the energy for transport and mixing in the inlet. The SSP data provide an estimate of the tidal energy. A least-squares harmonic analysis of the records in the east and west channels was performed (Table 2) for seven tidal constituents, two of which are shallow water constituents.

Except for the fact that the root mean square amplitude of the tide was slightly greater at the west site, there were no significant differences in the tide at these two locations. The M_2 tide arrived at the east channel site about 8 min before it arrived at the west channel site. Diurnal inequalities were essentially the same. Tidal asymmetries as a result of nonlinear generation of the M_4 tide were negligible, and the difference in phasing is probably not meaningful. However, a lack of asymmetries in elevation does not mean that the tidal currents themselves lack asymmetries. In fact, NEAP 1 anchor station data showed that currents accelerated to maximum ebb velocities within 1.5 h after slack water, with a prolonged ebb flow (elapsed time more than one-half the M_2 tidal period). The long duration of ebb is probably more a result of falling water levels in the inlet than of nonlinear generation of shallow water tides.

Response of sea level to wind stress

Cross-spectral analyses of the wind stress and SSP time series (Fig. 3) confirmed that the response characteristics discussed already were essentially the same in both channels (Fig. 5). The wind component axes were rotated in intervals of 15° to determine the wind component that was correlated with maximum response of SSP. When the east and north wind stress components were rotated along the principal axis of 57°, the maximum coherence squared along the major axis component exceeded 0.8, while that of the minor axis was not significant at the 95% confidence level (Fig. 5). The phase lag in the frequency intervals that contained maximum energy density in sea level (Fig. 4) was +108°, or about 1.2 days for frequencies of 0.25 cycle per day. This means that the north-eastward/south-westward wind stress was correlated with maximum set-down/set-up of the sea level. A separate analysis (not shown) revealed that another optimum direction occurs for wind stress with a direction of 15° east of north. This direction lies along a line which closely parallels the channel axis of Core Sound. The wind stress with a 'south' component along this axis was also accompanied by increased SSP in Beaufort Inlet.

There was a clear response of sea level (SSP) in the east and west channels to wind stress (Fig. 3). Five wind

Table 2. Tidal harmonics derived from the SSP records in the east (Shackleford Bank) and west (Fort Macon) channels.

	Amplitude (m)		Phase (degree)	
	East	West	East	West
M_2	0.430	0.488	114	118
S_2	0.083	0.097	147	149
N_2	0.073	0.084	331	334
O_1	0.047	0.052	335	335
K_1	0.042	0.046	163	159
M_4	0.006	0.006	125	94
M_6	0.005	0.006	67	52
RMS amplitude	1.34	1.38		
Derived parameters		East	West	
$(K_1 + O_1)/(M_2 + S_2)$		0.17	0.17	
M_4/M_2		0.014	0.012	
Phase $(M_2 + 2M_4)$		4	306	

RMS, root mean square.

regimes have been highlighted during the period 5 March to 18 April 1996, which illustrate the draining and filling of the inlet complex. Regimes 1 and 3 show that onshore wind stress was accompanied by decreases in sea level between 0.1 and 0.4 m in both channels. Regimes 2 and 4 followed these events with strong southward and south-westward wind stress, respectively, and sea levels increased by 0.2–0.4 m. Regime 5 was characterized by relatively rare south-eastward stress, which appeared to have a relatively small effect on the sea level. The sea-level responses to fluctuating winds are probably a combination of Ekman-induced transport of water across the shelf and direct down-wind transport of water through Core Sound and the Newport estuary complex.

Water-level differences between the east and west channels revealed that the wind set up significant barotropic pressure gradient forces between the two sites (Fig. 3(d)). Site separation was about 4 km and

Figure 5. Cross-spectra of wind stress components and SSP in the east and west channels, showing rotated wind stress (CLKN7) versus sea level for winter 1996: (a) coherence squared; (b) phase. Wind stress components are based on an *x*, *y* coordinate system rotated +57° counterclockwise from east.

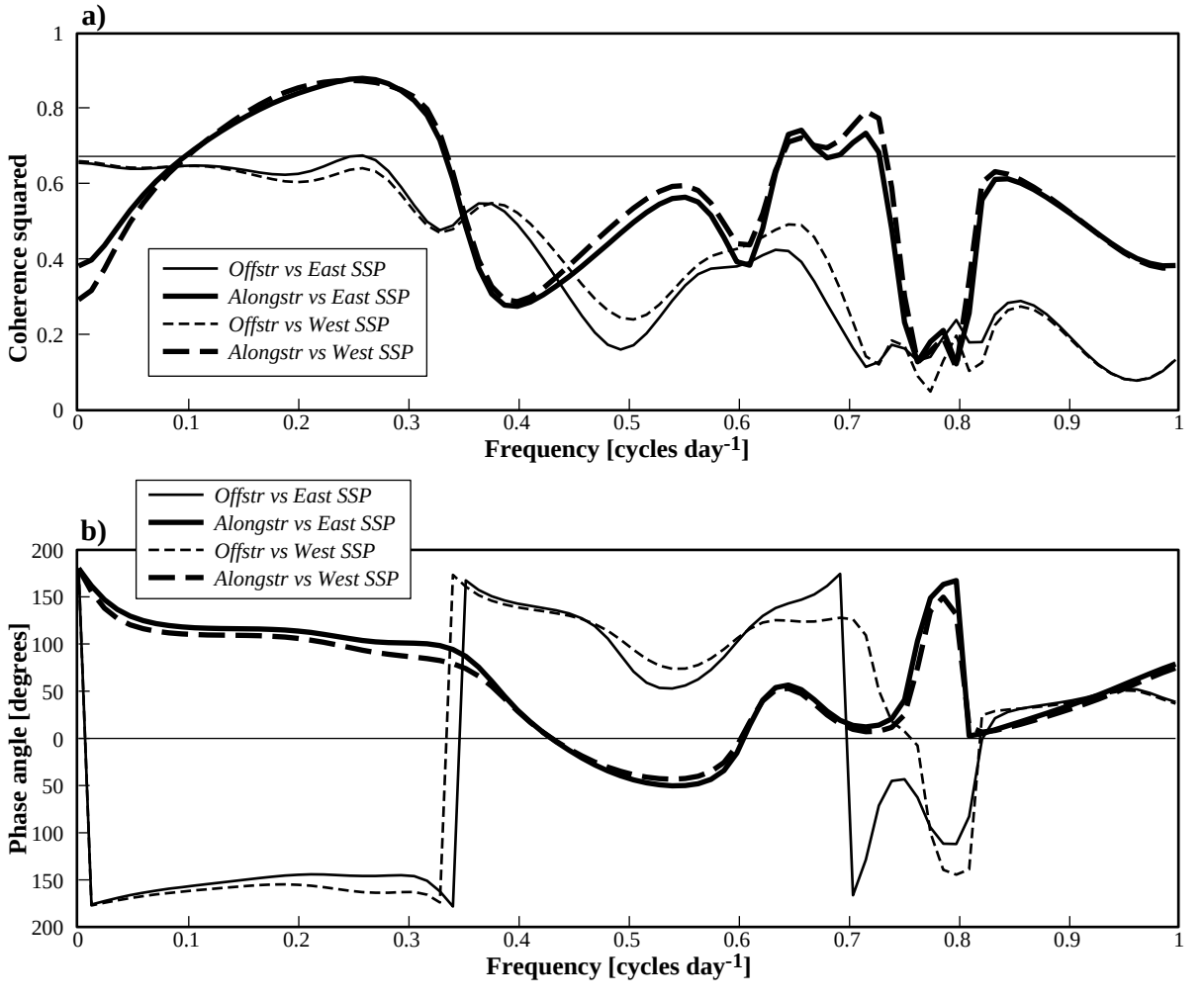

water-level differences reached maxima of about 0.05 m, and equivalent slopes were 0.05/4000 or 1.2×10^{-5}. Although the strong south-westward wind stress of 8–14 March caused the sea level to rise at both locations, the difference was sufficient to set up slopes of this magnitude. Opposite slopes occurred in association with north-eastward stress (20 March and 5 April), despite the fact that the sea level was set down at both locations.

One expects sea-level set-up from Ekman fluxes as a result of south-west stress along a coastline that trends north-eastward, but one may also expect that some volume of water will be blown down Core Sound into the east channel. It is important to determine the relative importance of volume fluxes from Pamlico Sound into the study area, since there is ample evidence that wind set-up in the sound can drive water into the Beaufort Inlet area (Pietrafesa and Janowitz, 1988). Therefore, despite wind-generated set-up and set-down of sea level throughout Beaufort Inlet, significant barotropic pressure gradient forces occurred between the two sites. The force was westward toward Bogue Sound for south-west wind stress. For stress to the north-east, the force was eastward toward Back Sound (and Core Sound). This is consistent with the following: (i) winds from the north-east blowing water through Core Sound and into Back Sound and slightly raising the sea level at the East site; and (ii) winds from the south-west blowing water down Bogue Sound and slightly raising the sea level at the west site.

The response of the sea level in the inlet to wind events has an important effect on the durations of the flood and ebb portions of the tidal cycle. Falling sea level is expected to extend (shorten) the duration of ebb (flood) tides. This appears to be the case for north-eastward wind stress in Onslow Bay. In contrast, south-westward stress should increase the sea level, which would shorten the relative duration of ebb tides.

Salinity and temperature response to winds and tide

Examination of the temporal fluctuations in salinity and temperature in the east and west channels (Fig. 6) reveals a complex response to the tide and wind regime. At the beginning of the record, tidal salinity fluctuations were more or less uniform in both channels, until there was a change to onshore wind stress (less than 0.1 Pa), which lasted about four days (event marked '1' in Fig. 6). The amplitude of salinity fluctuations decreased in the east channel. Temperature fluctuations were small in both channels. This indicates that the ebb tide in the east (west) channels advected water of relatively high (low) salinity past the sensors. The dampened salinity fluctuations in the east channel occurred during similar events of onshore wind stress (20–21 March; 4–6 April; 12–29 April), many of which also had a eastward component. It appears that these wind stress regimes shut down the supply of low-salinity water in the east channel, while having relatively little effect on the supply of low-salinity water in the west channel.

One of the strongest wind events (greater than 0.3 Pa) occurred on 9–13 March (Fig. 6, event 2). The air temperature dropped from 15 °C to 0 °C during the first two days of the event. Wind stress was south-eastward to south-westward (downwelling-favourable on the continental shelf), and tidal fluctuations in salinity increased in magnitude first in the west channel, followed by increased fluctuations in the east channel. Maximum fluctuations of greater than 15 PSU occurred in the west (east) channel three (four) days after the onset of this event.

A similar but weaker wind event occurred between 27 March and 3 April, during which salinity fluctuations also increased in both channels. However, the increase in the east channel was much smaller than that which occurred there during the event on 9–13 March.

Clearly, wind stress from the north supplies lower salinity water into both channels, but appears to supply more to the west channel in a shorter period of time. The exception was the first south-westward stress event when lowest salinity actually occurred in the east channel and lagged low salinity in the west channel by one day.

Changing winds and air temperature played key roles in governing the temperature and salinity of water in the two channels. The water temperature was relatively warm during event 1 (Fig. 6). From 10 to 14 March, there was a strong positive temperature–salinity correlation in both channels (low temperature correlated with low salinity), indicating that low-salinity estuarine water was colder than high-salinity ocean water. This correlation was amplified significantly during event 2. (Even ocean water cooled enough to produce a low negative correlation at high water.) Once event 2 ended, low water temperature in both channels increased, so that low salinity at low tide was correlated with warmer than average temperature. Between 22 and 26 March, the temperature in both channels fluctuated with a 24-hr period, reflecting diurnal heating rather than tidal advection of a temperature gradient. The fluctuation periodicity gradually changed to 12.4 h as the warmer estuarine water mixed with the relatively colder, higher salinity ocean water.

Upwelling-favourable winds blew for the final eight days of the record (Fig. 6, event 6). Fluctuations in salinity had decreased significantly to be replaced by relatively large temperature fluctuations. The fluctua-

Figure 6. Cape Lookout wind stress, salinity and temperature in the east and west channels from 4 March to 18 April 1996: (a) wind stress; (b) salinity; (c) temperature. Shaded areas denote events discussed in the text.

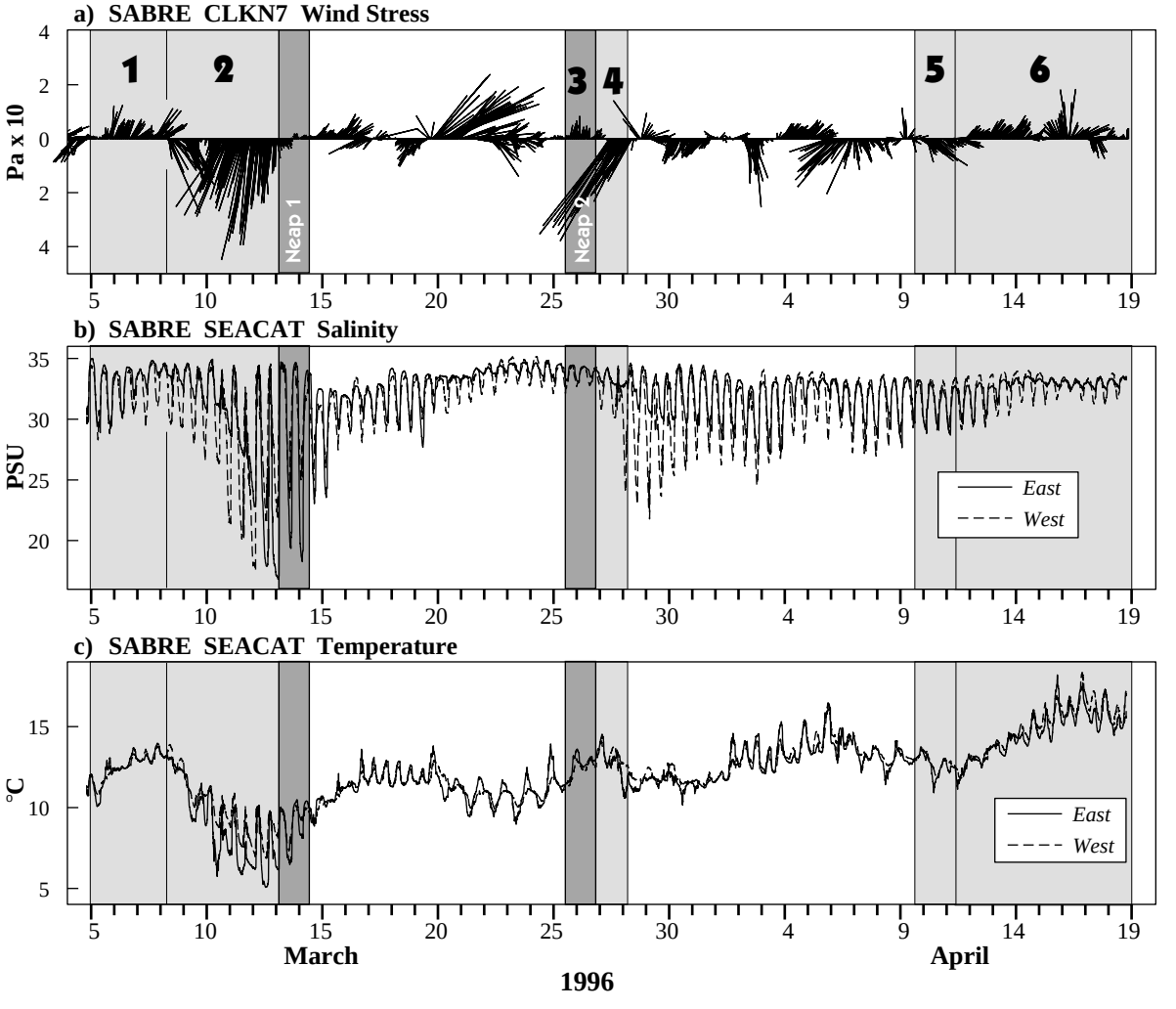

tions were somewhat larger in the west channel, suggesting that the fresh-water source in the Newport River created lower salinity than did the more remote fresh-water source of Pamlico Sound in the east channel.

The preceding discussion will now be used to set into context the conditions encountered during NEAP 1 and NEAP 2 intensive sampling periods.

Conditions leading to NEAP 1

During the strong north-easter of 8–13 March (Fig. 6, event 2), salinity fluctuations in the west channel increased significantly, followed by corresponding fluctuations in the east channel about a day later. Salinity ranges during a tidal excursion exceeded 15 PSU and salinity fell below 20 PSU at both locations. The salinity regime returned to prestorm conditions by 16 March.

The water temperature fell by about 5 °C during event 2 and by 3–5 °C for the four days leading up to NEAP 1. The highest temperature occurred at high water, indicating that estuarine waters were about 5 °C colder than oceanic waters. Semidiurnal temperature fluctuations were strongest in the east channel.

Subtidal fluctuations in SSP (Fig. 3(c)) indicate that the sea level in both channels increased by about 0.5 m after the onset of north-easterly winds. After the storm abated, water drained from the estuarine system, as indicated by the decrease in SSP during the period between 14 and 16 March. The sea level also appeared to be about 3–5 cm higher in the east channel.

Thus, the NEAP 1 experiment was conducted during a period when (i) the lowest salinity values in both

channels were recorded and (ii) subtidal sea level was decreasing in both channels.

Conditions leading to NEAP 2

Tidal frequency salinity and temperature fluctuations in the 10 days prior to NEAP 2 were much less than for the conditions leading up to NEAP 1 (Fig. 6). Salinities between high and low water varied by about 5 PSU between 16 and 20 March, but fluctuations decreased to less than 2 PSU immediately preceding NEAP 2, from 20 to 25 March. Salinity increased in both channels during the period from 15 to 25 March, reaching a mean value of about 34 PSU in both channels (Fig. 6(b)).

The tidal frequency temperature fluctuations were greatest in the east channel, suggesting a larger longitudinal temperature gradient. Note that the phasing of temperature fluctuations changed during this period. At first, the high-water temperature was about 1° C lower than the low-water temperature, indicating that the ocean water was slightly cooler than the estuarine water. The phasing in temperature became rather confused in the period from 20 to 29 March, suggesting weak along-channel temperature gradients.

Subtidal SSP changes indicated a decrease in water level in both channels beginning on 19 March and lasting until 21 March (Fig. 3(c)). The sea level rose during the period from 21 to 24 March, after which it levelled off. Thus, the NEAP 2 experiment was conducted during slightly decreasing sea levels in the channels and when salinities were relatively high and steady over a tidal cycle.

Definition of ocean temperature and salinity

The temperature and salinity in both channels were examined at the time of high water in order to define the characteristics of ocean water advected into Beaufort Inlet during flood tide. The east and west channels would actually withdraw ocean water with different salinities based on the supposition that the withdrawal zones for each channel would have different amounts of fresh-water content from the previous ebb tide. High-water 'ocean' values were defined as those occurring 1 h after the time of highest pressure. This allows for the fact that each slack water usually occurs about 1 h after high or low water.

Ocean salinity and temperature fluctuations based on the high-water analyses of both channels were compared with wind stress (Fig. 7). There were broad trends in these signals, which appeared to be related to wind regimes lasting two or more days. The ocean values were more or less steady at 34 PSU until the 9–13 March north-easter, when the ocean salinities dropped by almost 2 PSU. Ocean temperatures also fell by more than 2 °C during this interval. It is not certain if the ambient ocean salinities fell by this amount as a result of (i) advection of low-salinity water around Cape Lookout or (ii) advection of a mixture of low-salinity water that was in the plume which exited the inlet. In any case, salinities increased quickly to prestorm values immediately after the storm abated and subsequently fell again with the onset of weak upwelling-favourable winds which would bring in water from the west along the coast. If the preceding north-easter had advected a band of low-salinity water westward along the coast of Onslow Bay, then the return to low salinity values following the wind shift would be consistent with this.

These low ocean salinities returned to values greater than 34 PSU as the upwelling-favourable wind regime continued until 24 March. The ocean salinities gradually decreased from 24 March to 10 April (a period when the wind record consisted of five north-easters with short interludes of upwelling-favourable winds). The north-easters would presumably advect low-salinity water around Cape Lookout. The ocean salinities increased again at the end of the record as upwelling-favourable winds commenced (Fig. 7).

In summary, the oceanic salinities fluctuated mainly between 33 and 34 PSU, with occasional departures to lower values. However, during NEAP 1 and NEAP 2, the ocean salinities were about the same at 34.4 PSU. After the storm on 9–13 March, the ocean temperature increased from 10 to 16 °C on 18 April. Even so, the ocean temperature during NEAP 1 was only 1 °C cooler than that during NEAP 2. This means that processes occurring within the estuarine complex governed the temperature and salinity conditions more than did fluctuations in the ocean adjacent to the inlet.

RESULTS OF NEAP 1 AND NEAP 2 EXPERIMENTS

Comparison of currents, temperature and salinity at larval abundance sites

The surface and bottom temperatures and salinities were analysed at all larval abundance sites in order to determine intersite similarities and differences (Table 3, Fig. 8). These analyses indicate clear differences between NEAP 1 and NEAP 2. At all sites during NEAP 2, the water temperature and salinity ranges were only 2° C and 2 PSU. The overall ranges of observed temperature were slightly greater during NEAP 1. In contrast, salinity was dramatically different, and our site comparisons will be confined to NEAP 1 salinities when fluctuations were significantly greater.

Figure 7. High-water (HW; oceanic) values of salinity and temperature in the east and west channels compared with Cape Lookout wind stress: (a) wind stress; (b) HW salinity; (c) HW temperature.

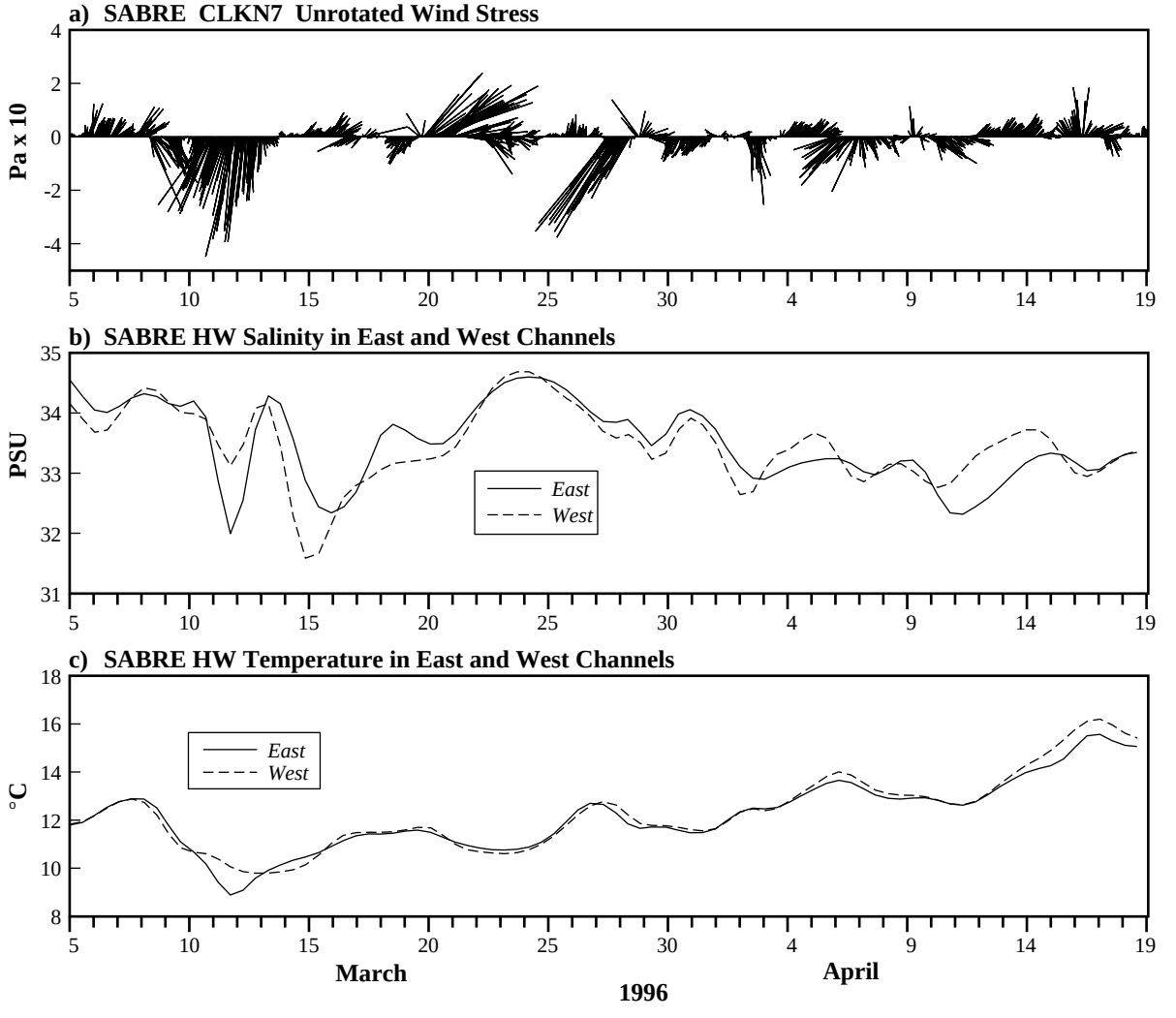

During NEAP 1, the salinity was as low as 19 PSU in the east channel (Fig. 8) and there was a larger degree of vertical stratification. The least vertical stratification was observed in the small channel leading to Beaufort (R/V Cable, Fig. 8). High-tide salinity, vertical gradients, as well as the fluctuation in salinity during the tidal cycle, were generally less there.

The greatest high-tide salinity was observed on the bottom in the inlet throat, followed by the east and west channels and the channel into Beaufort. The greatest vertical gradient at low tide was in the west channel and the inlet throat. Interestingly, the lowest low-tide salinity at the surface and bottom was observed in the east channel, raising the question as to its source.

Next, the currents and salinity variations in the east and west channels are compared for NEAP 1 and NEAP 2. The currents were significantly stronger at the east site during both experiments.

Conditions in the east and west channels

During NEAP 1, the salinity fluctuated between 19 and 35 PSU in the east channel compared with a range of 24–35 PSU in the west channel (Fig. 9(a)). The vertical salinity gradient was higher in the west than that in the east channel. There were brief interludes of salinity stratification at the east site at times near slack water. Stratification in the west channel was most pronounced after the maxima in ebb current. The ebb currents reached 1.4 m s^{-1} in the east channel compared with 1.0 m s^{-1} in the west channel. The flood currents were significantly weaker in both channels. Maximum vertical shear

Table 3. Maximum salinity (PSU) and temperature (°C) ranges near surface and near bottom observed during NEAP 1 and NEAP 2 at the four larval abundance sampling sites (see Fig. 1).

	NEAP 1 Salinity	Temperature	NEAP 2 Salinity	Temperature
Inlet (Onslow Bay)				
Surface range	22.2–34.0	8.1–10.4	33.6–34.8	11.7–12.8
Bottom range	30.5–35.0	9.5–10.4	34.0–34.9	11.4–12.8
East (Capricorn)				
Surface range	19.0–35.0	6.9–10.5	33.0–34.3	11.5–13.6
Bottom range	20.0–35.3	6.8–10.5	33.0–34.3	11.5–13.6
West (Hudson)				
Surface range	22.6–34.2	7.7–10.1	32.3–34.8	11.7–13.4
Bottom range	27.3–35.0	7.9–10.1	32.8–34.8	11.5–13.3
Channel (Cable)				
Surface range	24.8–31.7	7.7–10.0	33.0–34.8	11.7–13.3
Bottom range	25.5–33.5	7.8–10.0	33.0–34.8	11.7–13.3

Figure 8. Comparison of bin-averaged bottom and surface salinities at the four larval sampling sites during NEAP 1.

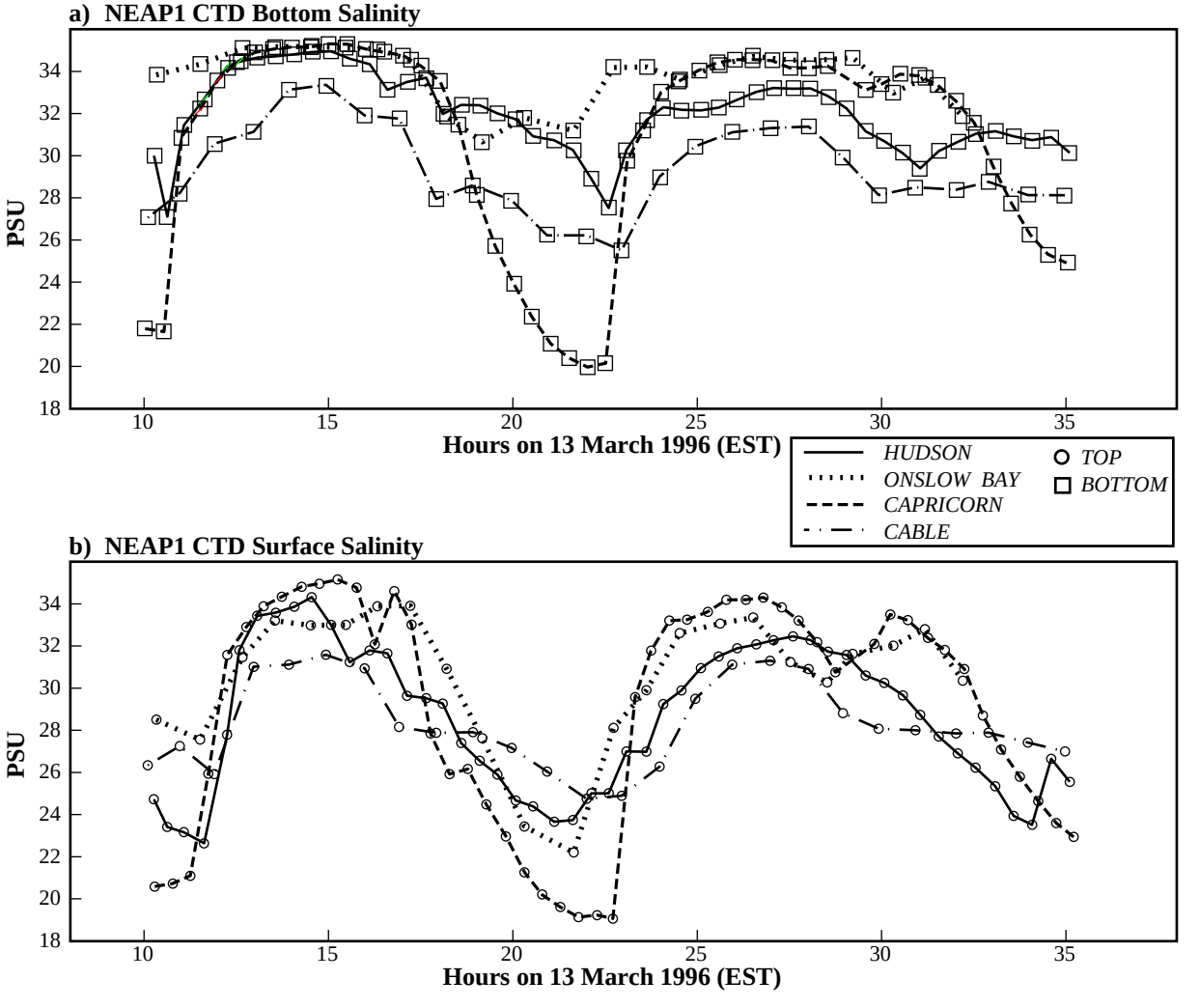

Figure 9. Comparison of currents and salinity at selected fixed levels in the west (Hudson) and east (Capricorn) channels during (a) NEAP 1 (13–14 March) and (b) NEAP 2 (25–26 March). Note different current and salinity scales for NEAP 2.

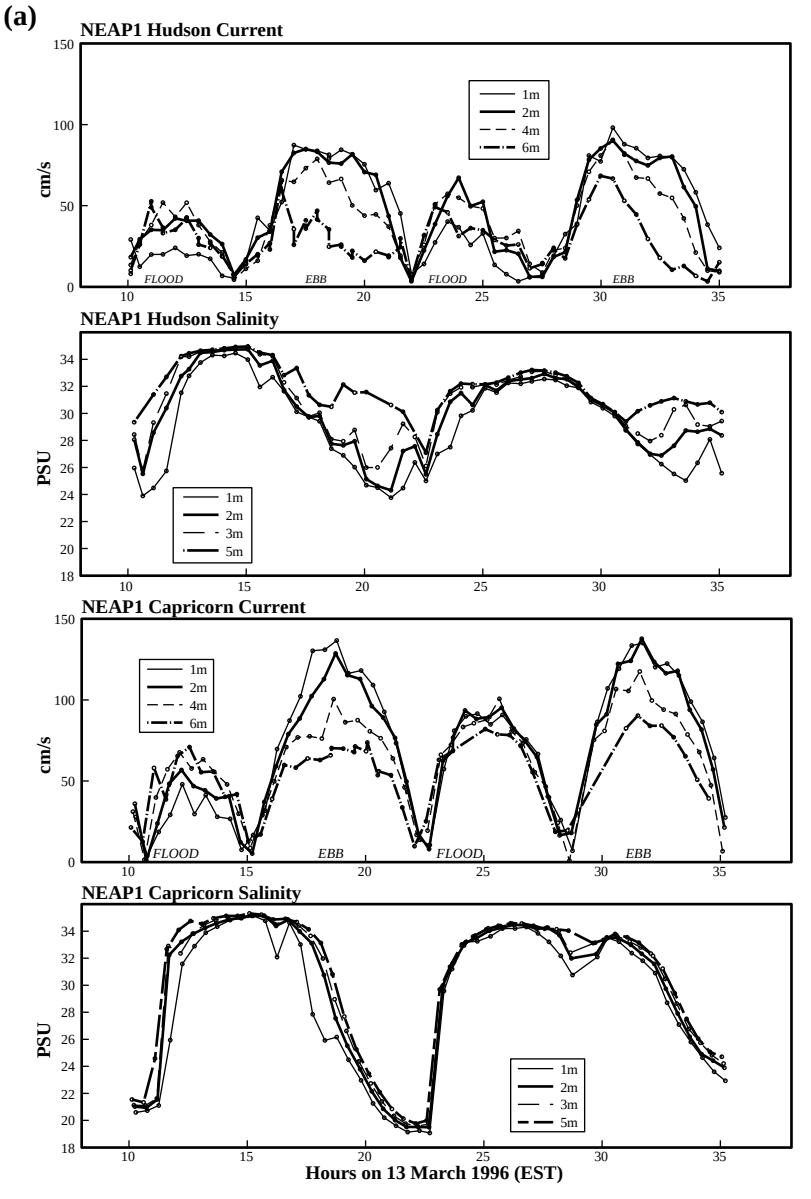

occurred in the west channel during ebb and generally occurred about an hour before the maximum vertical salinity stratification (Fig. 9(a)). Maximum vertical shear also occurred during ebb in the east channel, and there is no apparent correlation with vertical salinity gradient.

The NEAP 2 salinity fluctuations were much lower in both channels than during NEAP 1, and the low-tide salinity was significantly higher at both sites. The salinity fluctuated in the range 32.5–34.5 PSU in the west channel, and in the range 33–34.5 PSU in the east channel. Stratification in the west channel basically occurred at the end of the ebb through low water slack. The currents were generally stronger in the east channel but still smaller than at NEAP 1 at both sites (Fig. 9(b); note different vertical scales). Vertical shear in the currents was generally less at both sites during NEAP 2. However, while the maximum flood currents in the west channel were smaller than ebb during both NEAP 1 and NEAP 2, the maxima ebb and flood currents in the east channel were similar for NEAP 2.

Figure 9. (b)

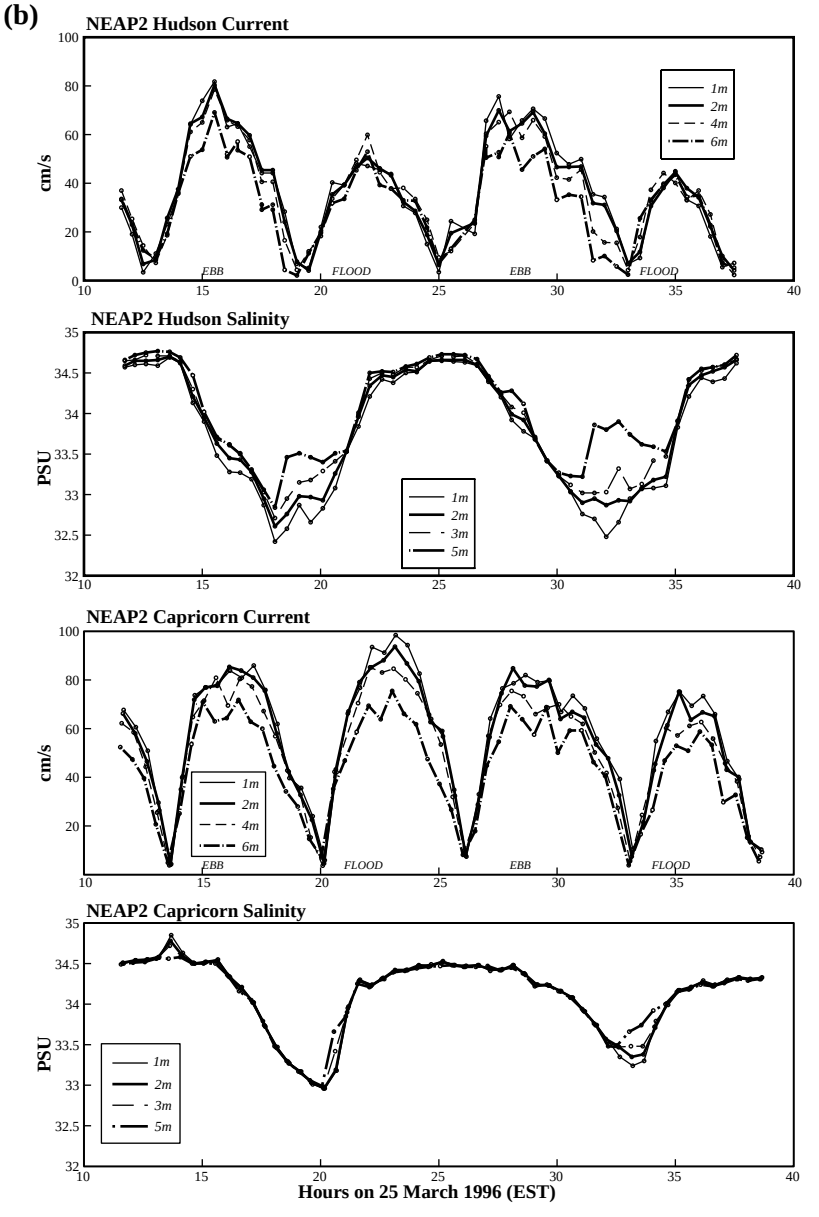

Conditions in the inlet throat

The cross-inlet differences in temperature and salinity were examined by comparing the temporal changes in surface and bottom temperature and salinity for the east, central and west stations in the inlet throat (Fig. 10). During NEAP 1, the greatest vertical stratification in temperature and salinity occurred at the central station, where the water was deepest. The high-tide values of surface temperature and salinity were more or less uniform across the channel, but there were cross-channel variations in both variables at the surface for all other portions of the tidal cycle. During both flood tides, the surface salinity was consistently lower on the west side by 1–4 PSU and somewhat cooler as well. During the first ebb tide, the salinity and temperature were slightly higher on the west side.

During NEAP 2, the cross-channel salinity and temperature differences were less than 1 PSU and 1 °C respectively. There was quite a systematic cross-channel variation in bottom salinity at low tide (Fig. 10(b), near hour 20), where the salinity was lowest on the west side, highest in the middle and intermediate on the east side. Surface salinity during both ebb tides was consistently lower on the west side, intermediate in

Figure 10. Comparison of salinity and temperature at the eastern, central and western stations in the inlet throat for (a) NEAP 1 and (b) NEAP 2. Bold lines connect bottom values. Note different temperature and salinity scales for NEAP 2.

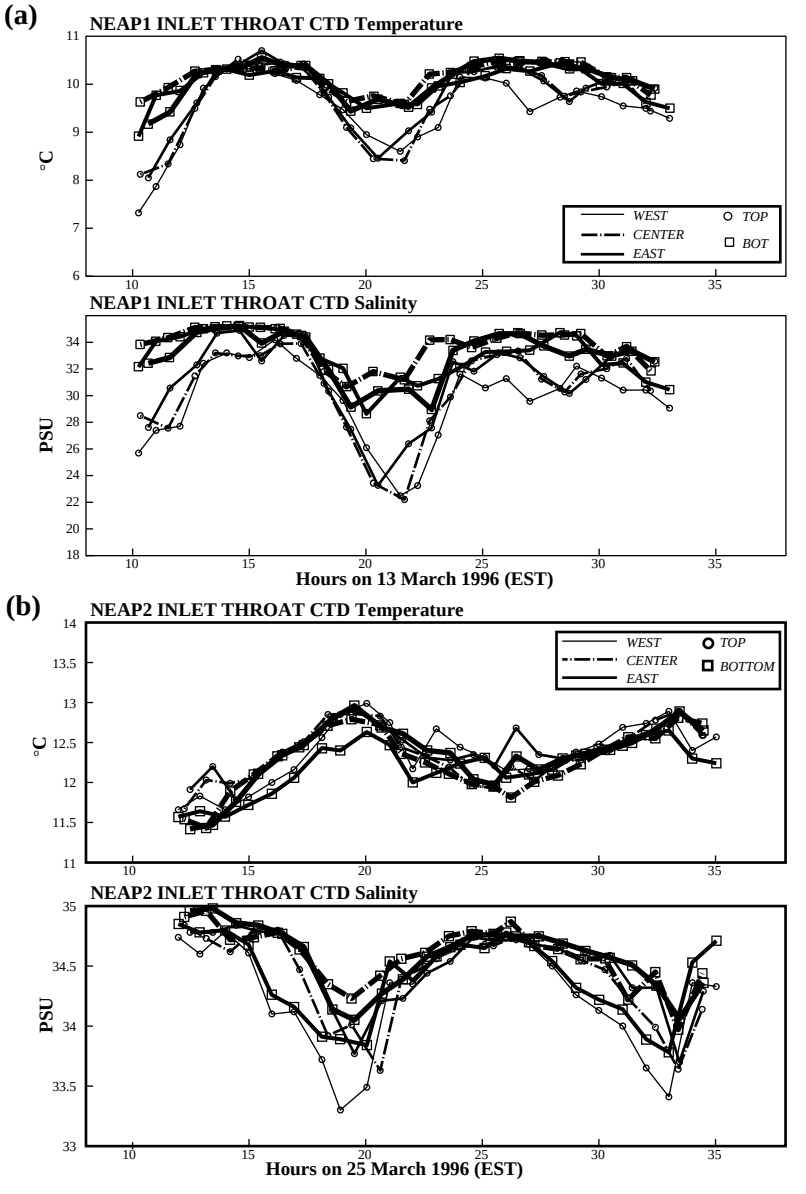

the middle and highest on the east. The differences were smaller and inconsistent during flood tides.

DISCUSSION

East- and west-channel tidal currents

The surrounding intertidal areas represent one of the distinguishing differences between the east and west channels. The east channel is bounded by extensive areas of tidal marshes fed by many small tidal creeks. In contrast, the west channel has a relatively 'hardened' boundary, because of port development.

The model of Fitzgerald and Nummedal (1983) based on conservation of mass predicts that time intervals between high water in the ocean and high water in tidal creeks are maximized by the inefficient drainage of marshes located floodward. This has the effect of prolonging (shortening) the duration of flood (ebb) currents if no other subtidal processes,

such as wind-induced draining or filling of the system, are occurring. Short-duration ebb currents are stronger than are flood currents—an effect labelled by some as 'ebb-dominance'. Table 4 indicates that high-water slack in the east channel occurred on average about 1 h later than did the corresponding interval in the west channel. However, the vertical tide (SSP) was in phase within 8 min (Table 4). The large phase differences in slack water are consistent with the fact that ebb currents are stronger in the east channel.

The tidal currents measured at the east anchor station were slightly greater than those in the west channel. The root mean square tidal amplitudes were within 4 cm of the same value (Table 2). Flood currents achieved their maximum values within 2 h of low-water slack (LWS) during NEAP 1 and within 3 h of LWS during NEAP 2. The wind stresses during the two experiments were within 0.05 Pa of the same strength, so we do not believe that wind stress accounts for the asymmetric behaviour of the flood currents during NEAP 1. The ebb currents achieved their maximum values about 3 h after high-water slack (HWS) during NEAP 1 and NEAP 2, but the second maximum ebb in the east channel occurred only 2 h later.

Table 4. Time intervals (h) relative to the preceding LW or HW in the east and west channels.

	NEAP 1 (13 March)		NEAP 2 (25 March)	
	West	East	West	East
LWS	2.25	2.63		
MF	4.50	4.33		
HWS	1.50	2.33	1.73	2.60
ME	5.00	5.67	4.33	5.60
LWS	1.00	1.33	1.08	1.90
MF	3.00	4.40	4.00	5.07
HWS	1.20	2.40	1.07	2.17
ME	4.50	5.60	4.00	4.07
LWS	1.63	2.00	2.08	2.00
MF			3.80	5.00
HWS			1.33	2.42

Average time intervals (h) between various parts of the tidal phase

	Time interval		Time lag
Tidal phase	West channel	East channel	East–west
LW-LWS	1.61	1.97	0.36
LWS-MF	3.83	4.70	0.87
HW-HWS	1.37	2.38	1.01
HWS-ME	4.46	5.24	0.78

LW and HW times were determined from SSP measurements. HW, HWS, LW, LWS, ME and MF stand for high water, high-water slack, low water, low-water slack, maximum ebb and maximum flood respectively.

The time intervals of various parts of the tidal current cycle relative to the vertical tide (Table 4) suggest the influence of locally generated pressure gradients. These pressure gradients are related to different draining and filling rates of the small channels and marshes further inland. These, in turn, can alter the characteristics of the tidal current (Boon and Byrne, 1981; Fitzgerald and Nummedal, 1983; Shetye and Gouveia, 1992).

No claim is made for statistical significance for the data in Table 4, because of the small number of tidal cycles analysed. Nevertheless, the between-channel differences are consistent with morphological differences in the floodward direction along the two channels. Recall that the subtidal sea level was falling during both experiments, even though the NEAP 1 ebb-phase duration was longer than that of the flood phase (opposite to what is expected in an ebb-dominant system). This would prolong ebb currents until the sea level in the ocean rose enough to overcome the subtidal pressure gradient driving the lowering of the sea level in the area. This is a subtidal process that must be included in any attempt to classify an estuary, based on tides alone, as either flood- or ebb-dominant.

In summary, the strong ebb phase in the east channel is consistent with the relatively slow drainage of the surrounding intertidal areas, which sets up a strong ebbward pressure gradient as the tide falls near the end of the channel. The relatively solid boundaries upstream in the west channel inhibit, in a relative sense, the set up of the ebbward pressure gradient.

Transport of low-salinity water in the east and west channels

The fixed-point salinity observations directly relate to the advection of the along-channel salinity gradient. Since vertical gradients in salinity and velocity are reasonably uniform throughout the tidal cycle, a simple one-dimensional salt balance captures reasonably well the relationship between temporal and spatial salinity gradients, or

$$\frac{\partial S}{\partial t} = -U\frac{\partial S}{\partial x}$$

where S and U are vertical averages of the salinity and velocity respectively. The contrast of temporal and spatial gradients in S in the east and west channels indicates differences in the strength and longitudinal position of the larger-scale estuarine salinity structure. We expect this structure to be related to fresh-water

input to the channels, wind mixing, upwelling or downwelling on the continental shelf, and the phase of the fortnightly tide.

Beginning on 5 March, low- and high-tide salinity values were approximately 30 and 34 PSU, respectively, in both the east and west channels (Fig. 5). Wind stress was upwelling-favourable (north-eastward stress). This wind regime continued until 8 March, and the low-tide salinity values increased to almost 34 PSU in the east channel. This indicates that the along-tidal-stream salinity gradient became very small, while the salinity gradient remained relatively large in the west channel. As pointed out earlier, winds with an upwelling-favourable and onshore component appeared to shut off the low-salinity supply to the east channel.

The wind conditions which followed were downwelling-favourable. The low-tide salinity diminished to less than 20 PSU in the west channel, followed two tidal cycles later by low salinity in the east channel. Low salinity persisted longer in the east channel than in the west channel. However, the amount of low-salinity water which appeared in the east channel during subsequent downwelling-favourable wind events was considerably less.

A likely explanation of these differences may be the location of low-salinity sources in the Newport River and the Neuse River which empties into Pamlico Sound further north (Fig. 1). Neuse River water can be advected into Core Sound which connects to Back Sound (the east channel) behind Cape Lookout. Onshore and upwelling-favourable wind stress appears to diminish the supply of the low-salinity sources in both channels but, in particular, restricts the supply in the east channel. This suggests that wind stress to the north-east retards the ebb flow in both channels sufficiently to affect the low-salinity supply in both channels (east component in Back Sound; north component in Newport River).

During stormy winds from the north-east, low salinity water can be advected into both channels from both sources. This appeared to be the case during the first such event, when the salinity in the east channel reached the lowest recorded level. These winds could effectively transport Neuse River water along the south end of Pamlico Sound and into Core Sound, where the south-westward stress could advect the low-salinity water into the east channel. The plume presumably extends along the south shore of Pamlico Sound, and the strength of the plume reached its maximum following the high discharge period. The particularly strong wind stress of 0.4 Pa would induce water speeds of about 40 cm s^{-1} (40 km per day), assuming a drag coefficient of 2×10^{-3} and a water/wind speed ratio of 0.03. Such winds could move low-salinity water at the north end of Core Sound down the distance of 80 km to the east channel in about two days. This suggests that the ebb flow is increased by southward and south-westward wind stress, which increases the supply of low-salinity water to both channels.

The likely explanation of why such low salinities were not observed in the east channel during subsequent downwelling events is related to discharge from the Neuse River. Discharge had decreased by 50% by 20 March relative to the high discharge of late January and early February (Fig. 2). Needless to say, the strength of the low-salinity signal appearing in the east channel would be proportional to the salinity of water at the north end of Core Sound. The strength presumably diminished from 20 March to the next significant downwelling events which occurred on 27 March. Although the low-tide salinity did decrease in the east channel during this event, the magnitude of the decrease was significantly less than for the main event of 8–13 March.

Wind-generated transport that affects the supply of low-salinity water might affect the supply of larvae to the estuarine complex. The implication is that some of the larvae observed in the east and west channels, as well as the minor channel leading into Beaufort, could be supplied from Core Sound, which connects to Pamlico Sound and the North River, both of which could receive their larval supply from inlets along Raleigh Bay and north of Cape Hatteras. However, the results of Churchill *et al.* (1999) represent convincing evidence that most of the larvae sampled during this experiment did enter the complex through Beaufort Inlet.

Cross-channel water mass differences in the inlet throat

Model studies (Luettich *et al.*, 1999) and observations (Churchill *et al.*, 1999) of the flow field indicate that the flood tide carries through the inlet throat continental shelf water found off Shackleford Bank on the east side, and a mixture of continental shelf and estuarine plume water usually found west of the inlet. Our observations support the expectation that these different sources set up cross-channel salinity gradients during certain phases of the tidal cycle.

Cross-channel gradients in temperature and salinity were observed in the inlet throat, which were comparable with observed axial gradients in the east and west channels. The differences were greater during NEAP 1 and, within a given tidal cycle, tended to be greatest near the time of low-water slack for both experiments (Fig. 11). The lower salinity and temperature on the west side confirm that the tidal stream there advects the cooler and less-saline water from the

previous ebb of the Beaufort Inlet plume back into the inlet. The salinity of this plume was undoubtedly depressed and sent westward along the coast line during NEAP 1.

Differential advection of along-current density gradients by tidal currents can produce cross-channel density gradients which set up axial fronts (Nunes and Simpson, 1985). In Beaufort Inlet, the tidal stream sets up density gradients in the throat, through the advection on the east side of higher-salinity shelf water next to advection on the west of Beaufort Inlet plume water. The resulting cross-channel gradient during flood tide could produce axial convergence on the surface and divergence underneath. Through this process, larvae that ingress preferentially through the throat on one side or the other could be redistributed cross-channel.

CONCLUSIONS

Tidal currents were stronger in the east channel, and ebb currents were stronger than flood in both channels. The input of low-salinity water into the upstream areas of each channel was greatest during the first neap-tide experiment and resulted in significantly greater salinity fluctuations throughout a tidal cycle. Strong north-east winds coupled with high discharge from the Neuse River appeared to account for the abnormally low salinities observed early in the study period.

A careful study of phase lags between the local vertical tides and the times of slack water suggested that the morphology of the tidal marshes and creeks played a greater role in the east channel. The friction of the marshes and small tidal creeks causes relatively slow drainage of these systems during ebb tide, resulting in high-tide water being stored there for a longer period of time. This produces a higher-than-normal barotropic pressure gradient during ebb tide, which drives a strong ebb-tidal current and appears to be a reasonable explanation of the higher tidal currents observed in the east channel.

The tidal stream in Beaufort Inlet set up strong cross-inlet gradients, through the advection on the east side of higher-salinity shelf water and advection on the west side of Beaufort Inlet plume water. The axial fronts produced by differential advection of these two water masses might play some role in redistributing larvae present in one tidal stream to another.

ACKNOWLEDGEMENTS

We wish to thank the able captains and crews of the R/V Susan Hudson and R/V Capricorn for excellent seamanship and cooperation during NEAP 1 and NEAP 2. We are also grateful for the technical assistance of Kristen O'Malley and Jesse McNinch, both in the field and in conducting much of the data analysis. We thank Dr Richard Forward, Dr William Kirby Smith and Mr Quentin Lewis for their hospitality and for providing us with comfortable offices during our stay at Duke University Marine Laboratory. Finally, we are grateful to an anonymous reviewer for his/her constructive and helpful comments on the discussion section. This work was supported by the NOAA's Coastal Ocean Program (Grant No. NA16RG0481-01 to the Georgia Sea Grant College Program).

REFERENCES

Blanton, J.O., Amft, J.A., Lee, D.K. and Riordan, A. (1989) Wind stress and heat fluxes observed during winter and spring, 1986. *J. Geophys. Res.* **94**:10686–10698.

Boon, J.D. and Byrne, R.J. (1981) On. basin hypsometry and the morphodynamic response of coastal inlet systems. *Mar. Geol.* **40**:27–48.

Churchill, J., Forward, R., Luettich, R., Hench, J., Hettler, W., Crowder, L. and Blanton, J. (1999) Circulation and larval fish transport within a tidally dominated estuary. *J. Fish. Oceanogr.* **8**(Suppl. 2):000–000.

Fitzgerald, D.M. and Nummedal, D. (1983) Response characteristics of an ebb-dominated tidal inlet channel. *J. Sed. Pet.* **53**:833–845.

Forward, R.B. Jr, Reinsel, K.A., Peters, D., Tankersley, R.A., Churchill, J.H., Crowder, L.B., Hettler, W.F., Warlen, S.M. and Green, M. (1999) Transport of fish larvae through a tidal inlet. *J. Fish. Oceanogr.* **8**(Suppl. 2):000–000.

Hofmann, E.E., Pietrafesa, L.J. and Aktinson, L.P. (1981) Bottom water intrusion in Onslow Bay, N.C. *Deep-sea Res.* **28A**:329–345.

Janowitz, G.S. and Pietrafesa, L.J. (1980) A model and observations of time dependent upwelling over the mid-shelf and slope. *J. Phys. Oceanogr.* **10**:1574–1583.

Jennings, C.D., Willis, J.N. and Lewis, J.M. (1970) Hydrography of the Newport River estuary: a preliminary report. Estuarine Menhaden Research Annual Report to US Atomic Energy Commission (AEC 66-70).

Kirby-Smith, W.W. and Costlow, J.D. (1989) The Newport River estuarine system. UNC Sea Grant College Publication UNC-SG-89-04. Chapel Hill, NC.

Klavans, A.S. (1983) Tidal hydrodynamics and sediment transport in Beaufort Inlet, North Carolina. NOAA Technical Report NOS 100. US Department of Commerce, Washington, DC.

Logan, D.G. (1995) Oceanographic processes affecting larval transport in Beaufort Inlet, North Carolina. MSc Thesis, North Carolina State University, Raleigh, NC.

Luettich, R., Hench, J., Fulcher, C., Werner, F., Blanton, B. and Churchill, J. (1999) Barotropic tidal and wind driven larval transport in the vicinity of a barrier island inlet. *Fish. Oceanogr.* **8**(Suppl. 2):000–000.

Nunes, R.A. and Simpson, J.H. (1985) Axial convergence in a well-mixed estuary. *Est. Coast. Shelf. Sci.* **20**:637–649.

Pietrafesa, L.J. and Janowitz, G.S. (1988) Physical oceanographic processes affecting larval transport around and through North Carolina inlets. *Am. Fish. Soc. Symp.* **3**:34–50.

Shetye, S.R. and Gouveia, A.D. (1992) On the role of geometry of cross-section in generating flood-dominance in shallow estuaries. *Est. Coast. Shelf. Sci.* **35**:113–126.

US Geological Survey (1996) Water resources data—North Carolina. Water year 1996. *Water-data Report NC-96-1*.

Weber, A.H. and Blanton, J.O. (1980) Monthly mean wind fields for the South Atlantic Bight. *J. Phys. Oceangr.* **10**:1256–1263.